Extended Detailed Finite Element Analysis of a 9.6 Metre Autogenous Sag Mill

John Hadaway
ANI PRODUCTS
1st Floor, 18 Miles Street
Mulgrave, VIC 31790 Australia

Eric Hecht
COMPUMOD Pty. Ltd.
309 Pitt Street
Sydney, NSW 2000 Australia

ABSTRACT

Finite element analysis is becoming an integral part of the design and manufacturing process of heavy engineering machinery for the mining industry in Australia. The Grinding Mill division of Australian National Industries (ANI) which is the division of ANI responsible for design, manufacture and supply of ore grinding mills to mines throughout Australia and overseas have been using the MSC/NASTRAN finite element analysis code extensively in all phases in the supply of their mills.

The finite element analyses of a 9600 mm diameter (5640 mm length) Autogenous Grinding Mill is used to describe how today's available technology is being used by one company to design and manufacture machinery for the mining industry.

EXTENDED DETAILED FINITE ELEMENT ANALYSIS
OF A 9.6M AUTOGENOUS MILL

TABLE OF CONTENTS

1.0 INTRODUCTION

The routine use of Finite Element Analysis is now well established in the design of major structures in minerals processing equipment. These models have been developed and calibrated to the point where they are reliable and cost effective and have allowed the designer to optimise material use and manufacturing processes. Australian National Industries (ANI) have developed standard design modelling approaches and these were described in detail at the 1990 MSC Users Conference.

In this paper we will discuss the use of Finite Element Analysis (F.E.A.) using MSC/NASTRAN to improve the detail design of a complex grinding mill structure. This paper will also discuss how F.E.A. is used to help evaluate manufacturing non-conformance with respect to variations in design which occurr during the manufacturing process. ANI has recently completed the design and manufacture of a large Autogenous Grinding Mill for use in a new processing plant at an Australian nickel mine. The mill is used in the particle size reduction of the nickel ore to allow the subsequent extraction and concentration of the mineral to nickel concentrate. The basic specification (Ref Fig 1) of the mill is as follows:-

- Autogenous mill (grinding mill with **no** separate grinding media)
- Diameter 9.6m inside shell
- Effective length 5.64m
- Operating speed 10.3 rpm
- Drive power 7000 KW
- Operating mass 1300 metric tonne

The increasing use of the Autogenous or Semi Autogenous grinding process combined with the requirements of operators for higher throughput has seen the physical dimensions of these machines increase dramatically over the last few years. In order to accommodate these demands and the limitations imposed by transport restrictions, crainage, foundry and machine tool limitations, it is necessary to make the main structures of the mill in more pieces (Ref Fig 2). The shell of this mill is manufactured in four pieces, as are the heads. Major bolted connections are therefore to be found in all directions. The shell is a combination of both radial and circumferential joints. The heads are comprised of a four piece radial segmented assembly. Including the two trunnions, the total number of pieces in the mill is fourteen.

2.0 Mineral Processing Mill Design and the Importance of MSC/NASTRAN 3D Finite Element Model in Stress Prediction

Mill suppliers around the world now make extensive use of finite element analysis in design. The modelling approaches vary and the two in most common use are 3D models of various types and axi symmetric 2D models. ANI has adopted the former as they feel it gives greater flexibility in the application of boundary conditions from such items as the internal charge loads, bearings and gearing. Also these models allow the introduction of non axisymmetric features which is extremely useful for studying the more detailed and unusual physical features of the machine. Some of the modelling discussed later would not be possible using an axisymmetric 2D or 3D model.

2.1 The Standard 3D Model of The Autogenous Mill

The standard ANI 3D mill model is used very routinely when submitting proposals to prospective purchasers of grinding mills and in the design activities of most projects. A common requirement is the inclusion of F.E.A. with the tenders. Generally, a confirmation analysis is conducted upon acceptance of the tender which incorporates any changes negotiated during the pre award stage.

The standard model assumes symmetry about the longitudinal axis and centre line of the mill and the internal charge load (or grinding mass) is modelled with a horizontal surface. The internal charge, its mass and resultant hydrostatic pressures assume an internal fill 5% higher than the maximum anticipated operating level. As this mill uses hydrostatic shoe bearings the bearing pressure is modelled as an even distribution over the bearing reaction area. In addition, a node at the centre of the bearing is connected by "soft" links to all nodes at the bearing surface and is fixed to remove vertical rigid body motion. The various assumptions inherent in the model have been tested by strain gauging mills over a range of mill types and configuration.

Using symmetry, only a quarter model of the trunnion, head and shell is required to be modelled and analysed. Solid 8 node HEXA elements are used to model the three components since they provide a good representation of the 3 dimensional stresses occurring in thick sections. These elements are used in large concentrations where high stresses are expected i.e. trunnion radius, journal radius, mill shell corner. In all other regions, the element density was chosen to ensure that the stiffness of the structure is modelled accurately. This typical model has approximately 14,000 nodes.

Figure 3 shows the quarter symmetric finite element model of the autogenous mill. Figure 4 shows the meshing detail in critical stress regions of the model. Typical stress range output is shown on a section of the mill in Figure 5. Contours of principal stress range (sigma1-sigma3) are used to assess fatigue prone regions in the structure. ANI has set strict criteria on the permitted range in the mill and the design is modified until the stresses are acceptable.

The bolted joints included in the standard model were the trunnion / head joint, the head / shell joint and the mill shell centre joint. These joints were modelled as fully bonded over the area of the seating face expected to remain in contact, and assume a complete transfer of load through the joint. A pressure load modelling the bolt preload is applied over a nominated effective region. The radial joints of the head and the longitudinal joints of the shell were not included in this model.

The steel liners of the mill were modelled as non structural mass spread over the mill shell, head and trunnion.

This model could be described as the standard ANI model and is used routinely in the design of new mill sizes and types. Various extended and more detailed models have been developed to investigate the complex structural connections inherent in large mills and manufacturing non-conformance.

2.2 The Extended 3D Model of The Autogenous Mill

In contrast with the standard finite element model of the autogenous mill, the extended model contains all radial and circumferential joints modelled in detail.

The extended model was developed to investigate the axial and radial bolted connections in the shell and heads of the 9.6m Autogenous Mill. The standard approach does not take account of these unsymmetrical features. The flanges are normally designed using manual methods and ANI felt further investigation using an F.E. model was justified to predict accurately the stress concentration effects around these flanges. To our knowledge this is the first time such an analysis has been performed by any mill manufacturers anywhere in the world.

The introduction of the non symmetrical joints added significantly to the size of the model. It was not the intention of ANI to make this model a standard design model but rather to investigate the structural behaviour of the joints and to establish design and layout rules to be used more generally in the development of new mills. The model is illustrated by Figure 6 and Figure 7.

The results of the analysis were largely uncontroversial with the exception of one area. At the inner end of the radial head joints we observed a significant concentration of stress which was brought about by the additional stiffness introduced by the flanges. The effect of adding stiffeners to a plane surface in bending is well known, however it is very difficult to predict with any accuracy the stress concentration effect which results. This model allowed ANI to do just that and in order to reduce the effect a series of simple detail models was used. The global information generated by the extended model was used as the boundary conditions. This investigation is discussed in the next section.

3.0 Detail Refinement To Determine Stresses In Critical Regions

The various detail investigations undertaken during the design of the 9.6m Autogenous Mill were developed on a case by case basis. In general the purpose of these was to optimise the shape of various parts in order to reduce the stress range in high stress areas and in part to optimise material usage.

The need to modify the details of the various components can be as the result of internal design requirements, customer request or sometimes at the suggestion of independent design auditors. The examples discussed here fall into those categories.

3.1 Radial Head Joints

As discussed in section 2.2 ANI identified an area of high stress at the inner end of the radial head joints. There was therefore, a need to optimise the end shape of the joints. The extended 3D model was very large and there was therefore significant time and cost involved in re-running and re-meshing the model. ANI decided that a simplified model was required that could be easily changed, geometrically, and run quickly and cheaply.

The solution was to use a simple 2D model of the region. This model was fixed at one end and at the other end a stress gradient was applied which was derived from the extended 3D model.

The model consisted of a 10 mm slice of a small portion of the top of the trunnion. This slice continued up into the head to a distance of approximately 400 mm from the beginning of the head flange. To represent the effective bolt preload region, no connection between the trunnion and head was assumed for a distance of 29 mm from the top of the trunnion. The loading on the model consisted of a force and moment obtained from results from the extended analysis and the bolt preload at the trunnion / head joint. Boundary conditions consisted of the bottom portion of the trunnion modelled fully fixed.

Figure 8 shows the mesh loads and boundary conditions applied to the model. The purpose of this was not necessarily to predict the actual stress but to establish the relative stress concentration of various options. A series of four trials were conducted which are summarised below.

Trial No	End Angle (deg.)	Radius (mm)	Stress Conc. Ratio
1	90	50	1.0
2	135	75	0.85
3	150	75	0.84
4	135	125	0.71

Table 1: Summary of radial flange model results

As previously mentioned the purpose of these models was not to predict absolute stress but to establish the relative merits of various geometric options. As the trial geometry corresponded to the original extended model, it is reasonable to say that by using trial 4 geometry we achieved an improvement in stress of around 29%. This magnitude of reduction is significant when designing fatigue sensitive structures near the maximum allowable stress range. (The stress range is the difference between the maximum and minium principal stresses and is used in fatigue life calculations).

3.2 Trunnion Extension

In response to a customer request to seek reductions in stress range in certain areas, ANI investigated a series of changes at the trunnion extension. Figure 9 shows the various geometrical options considered and table 2 gives a summary of the results.

Analysis	Model Description	LOCATION	
		Trunnion Radius (R15/R18/ R28/R50)	**Neck (Major Radius)**
3B	Trunnion liners not included, trunnion shoulder radius R15 (original run)	53.1	66.9
3B1	Trunnion liners included Trunnion shoulder radius R15	51.0	56.5
3B2	Trunnion liners included Trommel mass included Trunnion shoulder radius R15	52.6	55.5
3C	Trunnion liners included Trommel mass included Trunnion shoulder radius R18 20 mm decrease in trunnion liner diameter	51.1	52.1
3D	Trunnion liners included Trommel mass included Trunnion shoulder radius R28 Trunnion 27601D (75mm thick extension)	48.6	52.2
3E	Trunnion liners included (centre block omitted) Trommel mass included Trunnion shoulder radius R50, 53mm thick extension	53.1	55.5
3F	Portion of liners included, R50, 395 mm taper on trunnion extension, 2680 mm trunnion ID	43.2	52.2

Table 2: Summary of results trunnion extension radius

This series of analyses were conducted using the standard 3D model. This model does not usually include the trunnion liner and trommel which cantilevers off the end of the mill trunnion (refer to Figure 1) and is used in the separation process of the media. These items contribute small loads which are normally considered insignificant, and their omission from the geometrical model is generally conservative since stresses in the region of the trunnion where the trommel is coonnected are low. In this case the effect of these items was included in various ways to study their effect on the results, as it was thought that their inclusion might increase stresses at the trunnion extention radius.

3.3 Effect of Trunnion Liner & Trommel Screen

To be conservative in the modelling of the trunnion extension region, the trunnion liner and trommel screen were added to the standard model of the mill (refer to Figure 1). The moment on the trunnion due to the trommel mass acting as a cantilever on the trunnion in the trunnion extension region acts to open up the extension radius and therefore increase stress. Figure 10 shows the trommel and liner modelled.

Initially, the trommel screen and the trunnion liner were added to the model with the assumption that the trunnion liner was fully connected to the trunnion at three positions. The three positions were at the end of the trunnion extension, a centre block located near the inner trunnion journal radius and at the 15 degree inside sloping face of the trunnion. The 6 metric tonne mass (of the trommel) which is cantilevered off the trunnion was applied to the model at the end of the liner as a force and a moment. A number of analyses were performed using this model for various trunnion extension profiles and the results are shown in Table 2 above.

To further make the analysis conservative in the journal region, the trunnion liner connection to the trunnion was removed at the 15 degree sloping face as well as the centre block. (See Figures 11 and 12). In effect, all potentially adverse effects of the trommel screen and trunnion liner were modelled, and all beneficial effects were omitted from the model, so as to produce an upper bound stress range at the extension radius.

The results obtained satisfied ANI criteria and even more importantly, the client.

4.0 The Use of MSC/NASTRAN in the Manufacturing Process of Mineral Processing Mills

During the manufacture of a mill of this size non conformance with respect to the final design drawings can occur. These can be in various forms and often they are either on the boundary of the acceptance criteria and require detailed investigation to determine whether or not they of the acceptance criteria and require detailed investigation to determine whether or not they can be accepted. Others may be simple errors which occur during machining, and are simply not anticipated by the specifications and the initial design.

ANI uses FEA extensively in the evaluation of such non conformance. The model types adopted are designed to suit each case and the results are envisaged by independent experts in order to arrive at an appropriate course of action.

4.1 HEAD CASTING

During ultrasonic examination of the heads, some fine centre line shrinkage (fine porous structure) was found which was deemed to be marginally outside the ultrasonic specification. Due to the difficulty of performing ultrasonics on SG Iron a radiographic examination of the area was also carried out. This revealed that the areas were smaller than first thought and therefore acceptable.

It was decided, in any case, to take a closer look at the area and this was done by:-

1. Using F.E.A. to determine the likely stress concentration effect of the porous region.

2. Reviewing the individual porous defects at the maximum operating stress range using fracture mechanics methods.

The F.E. model was a modified version of the standard 3D model. An annular void of elliptic cross section (similar to the defect shape and size) was introduced which approximated the area in question. In other words no stress would be carried through the porous area. This is of course a very conservative approach as in reality the less sound material will have some stiffness, though it maybe less than the sound material. Also the use of a full annulus will increase the stress concentration effect by removing supporting, sound material around the area in question. This material would in practice support the area and help to reduce the stresses.

The model of the void area is shown in Figure 13. The stress concentration factor was demonstrated to be low and subsequent independent review using fracture mechanics concluded that there was minimal increase in the likelihood of failure occurring.

4.2 SHELL JOINT

During manufacture of the shell an error occurred in the drilling of the shell flange which connected with the head assembly. This left two extra holes mid pitch between bolt holes. A decision needed to be made as to the rectification approach.

A model of a section of the flange connection was made which used boundary conditions extracted from the standard 3D model. In order to realistically model the joint contact face, the model included non linear gap elements across all nodes on the contact surface of the joint. The MSC/NASTRAN non linear solution sequence 106 was used for the analysis. Results showed that the final stress range generated by the extra holes was well below the acceptable stress range design criteria and that the non conformance would not effect the structural integrity of the mill.

Figure 14 shows the finite element model.

5.0 CONCLUSION

The use of the MSC/NASTRAN finite element analysis code is a valuable tool which can be used for design and analytical purposes at all stages of a mill project. ANI started using MSC/NASTRAN purely as a design tool some years ago. The use of the technique has now been extended throughout the various stages including development of detail design and optimisation, and the evaluation of non conformance encountered during manufacturing. In combination with independent specialist advice a mill can be delivered with a high level of operational reliability. As with all such equipment it is the combination of the various fields of expertise which ensures a good final result. Finite element analysis and MSC/NASTRAN form part of this winning combination.

ani products Ruwalt AUTOGENOUS OR SEMI AUTOGENOUS GRINDING MILL

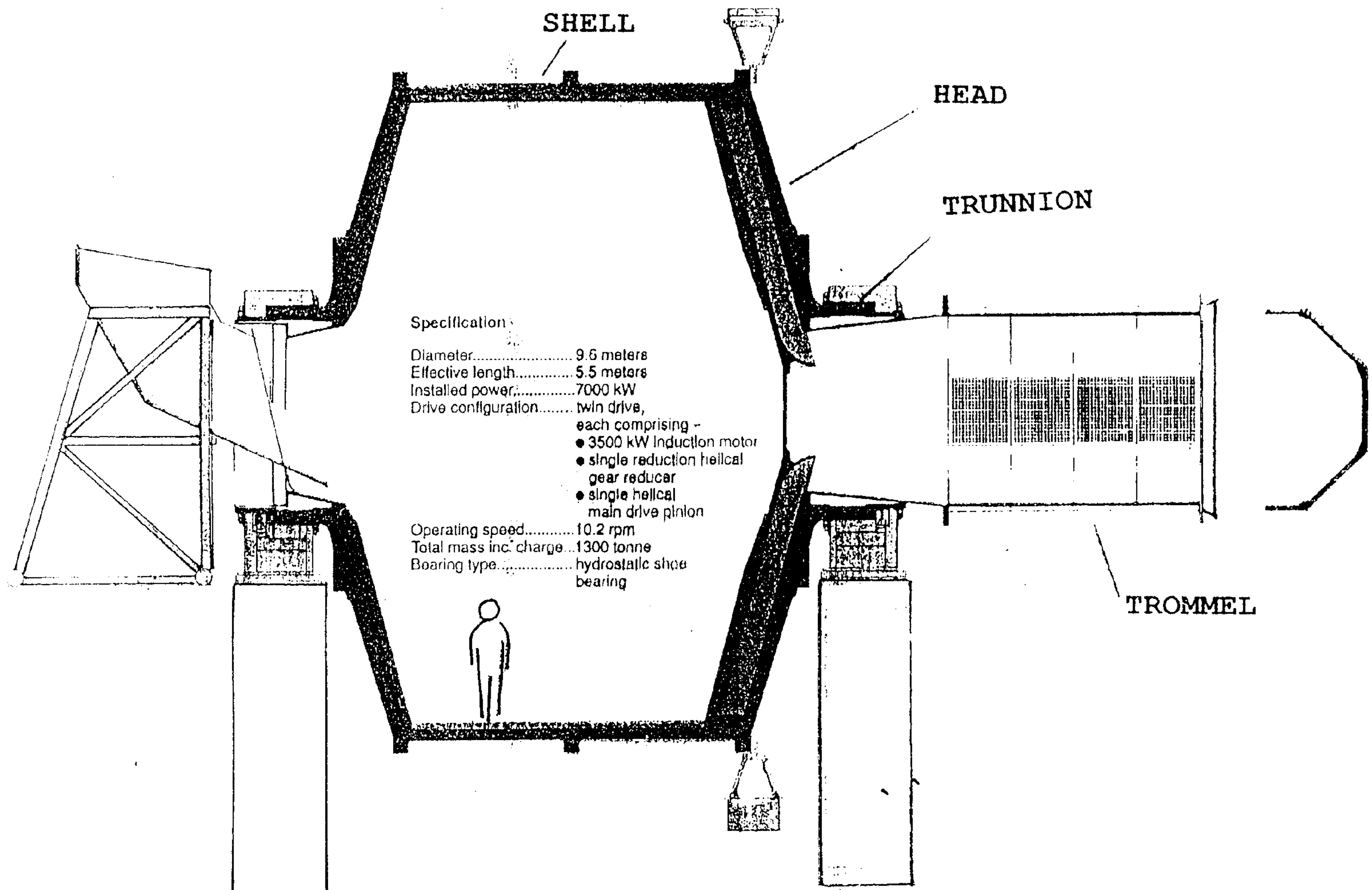

FIGURE 1

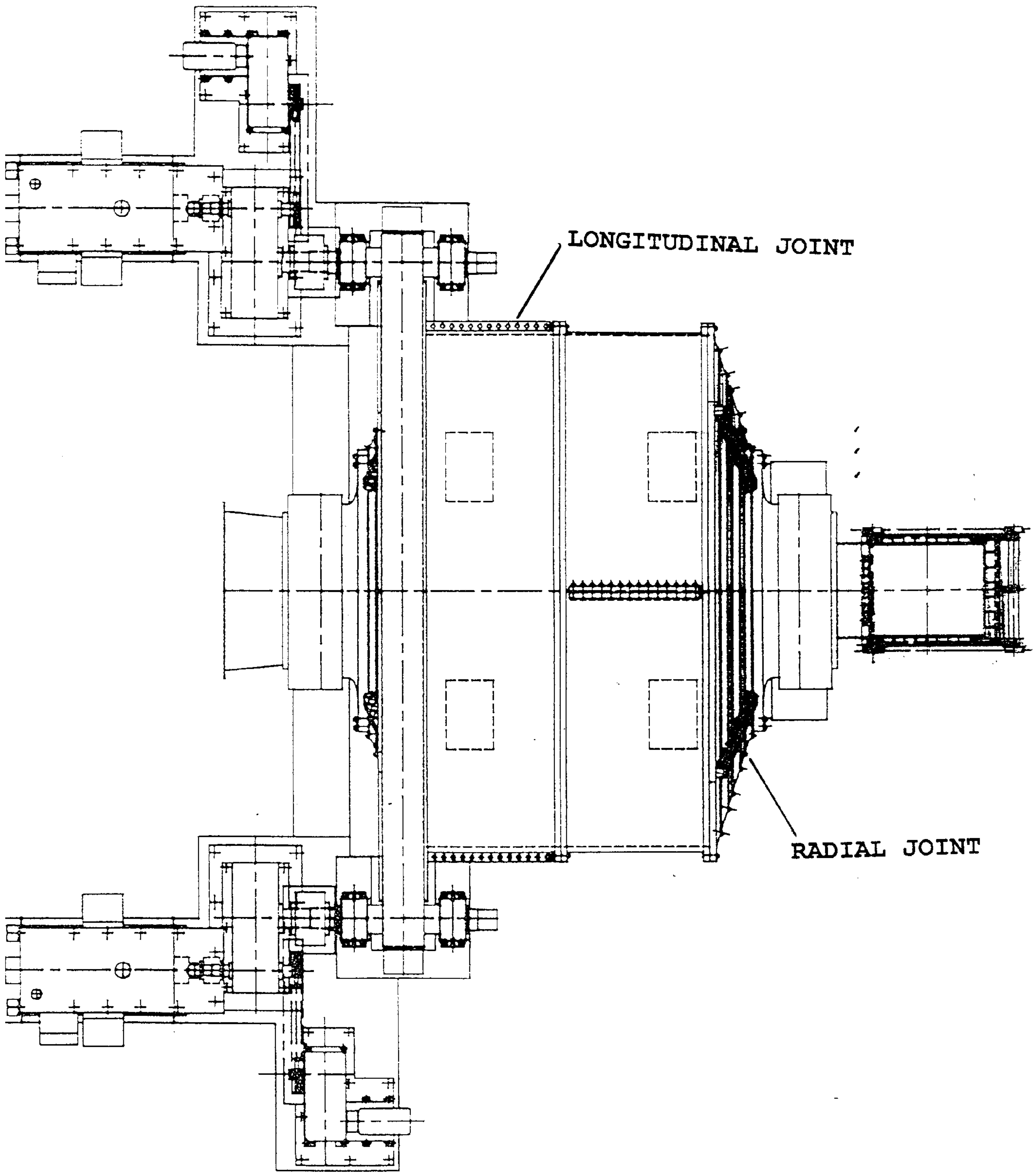

FIG 2

MILL JOINTS

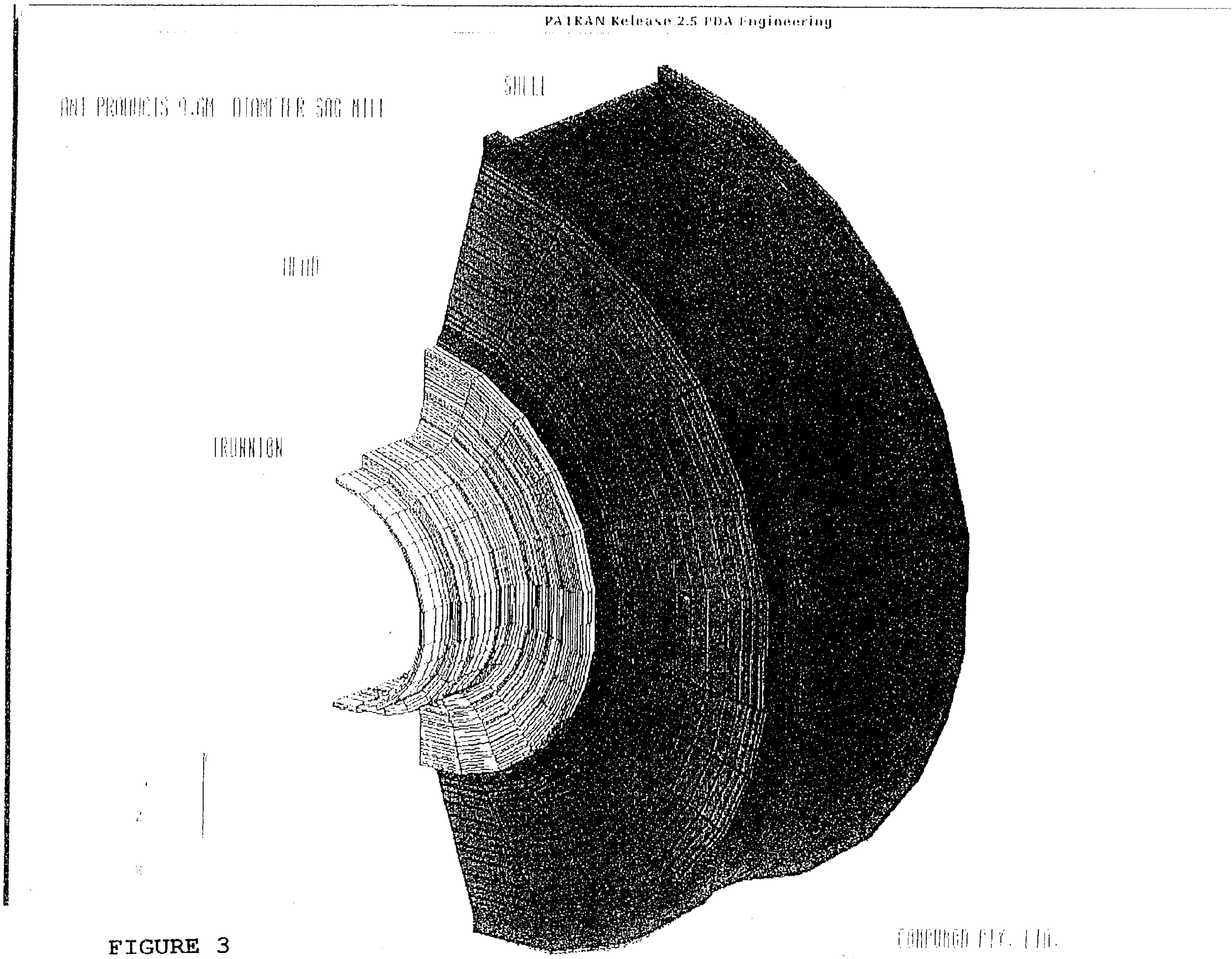
PATRAN Release 2.5 PDA Engineering
ANI PRODUCTS 9.6M DIAMETER SAG MILL
SHELL
HEAD
TRUNNION

FIGURE 3

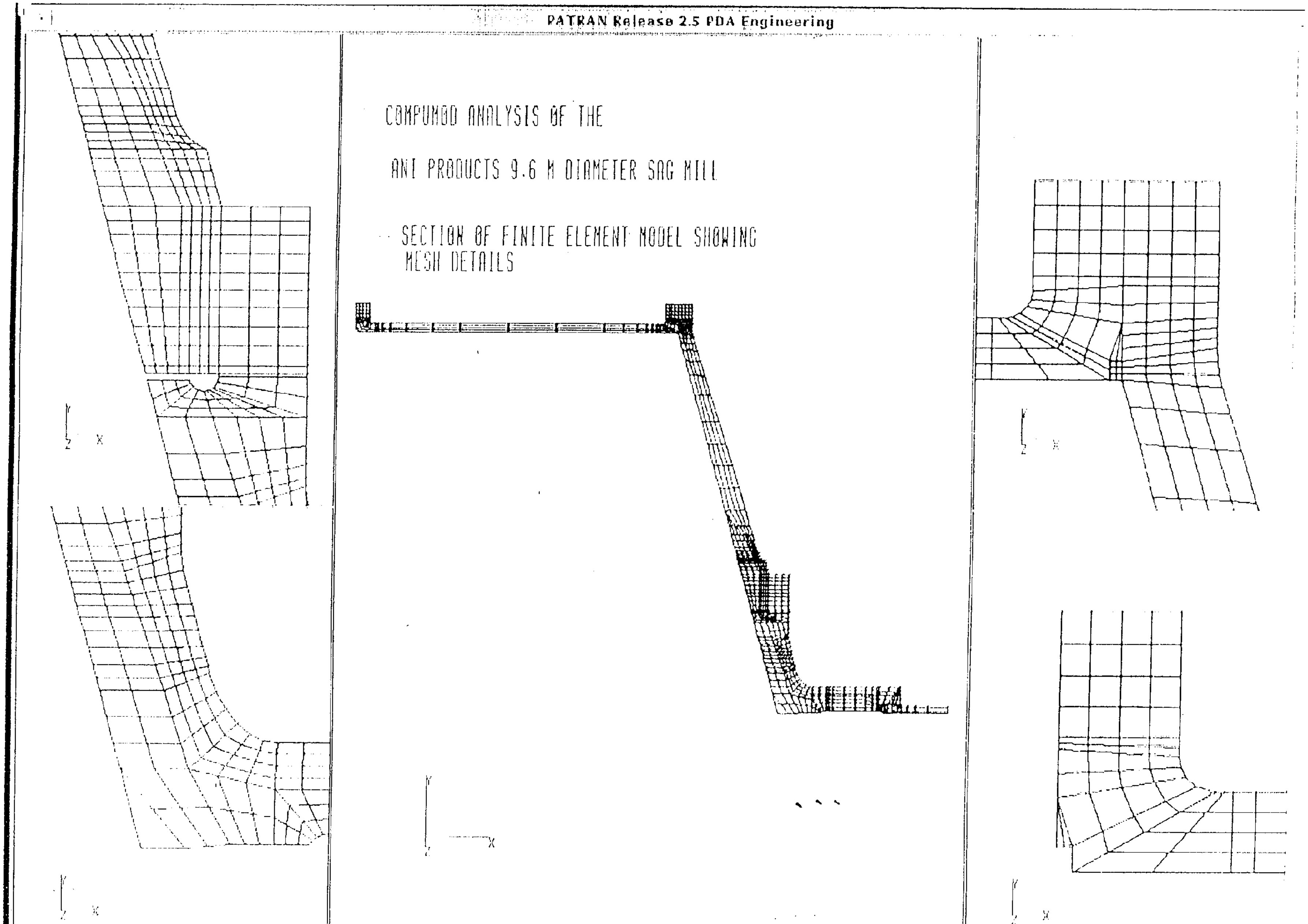
PATRAN Release 2.5 PDA Engineering
COMPUMOD ANALYSIS OF THE
ANI PRODUCTS 9.6 M DIAMETER SAG MILL
SECTION OF FINITE ELEMENT MODEL SHOWING
MESH DETAILS

FIGURE 4

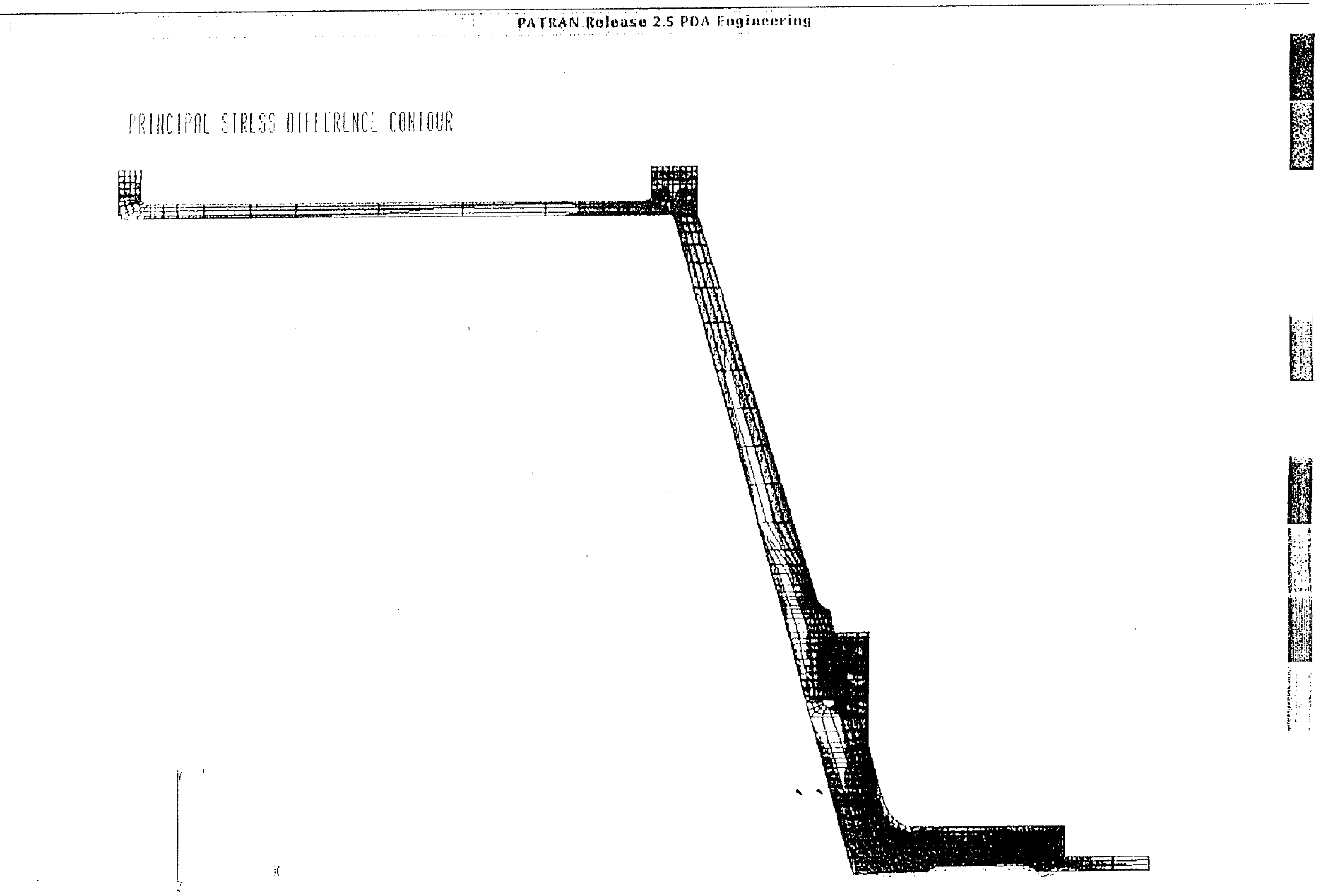
PATRAN Release 2.5 PDA Engineering
PRINCIPAL STRESS DIFFERENCE CONTOUR

FIGURE 5

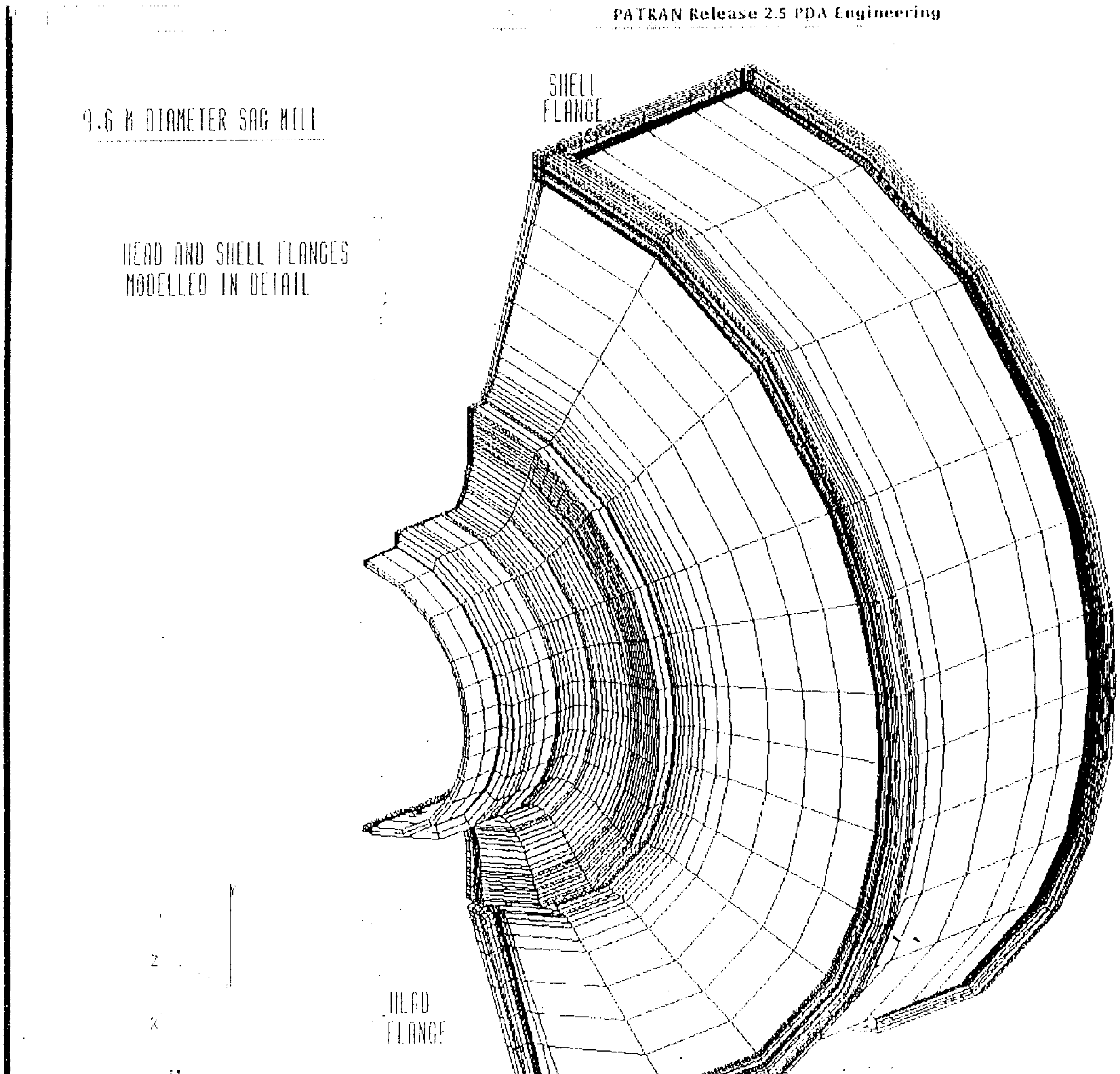
PATRAN Release 2.5 PDA Engineering
9.6 M DIAMETER SAG MILL
HEAD AND SHELL FLANGES
MODELLED IN DETAIL
SHELL
FLANGE
HEAD
FLANGE

FIGURE 6

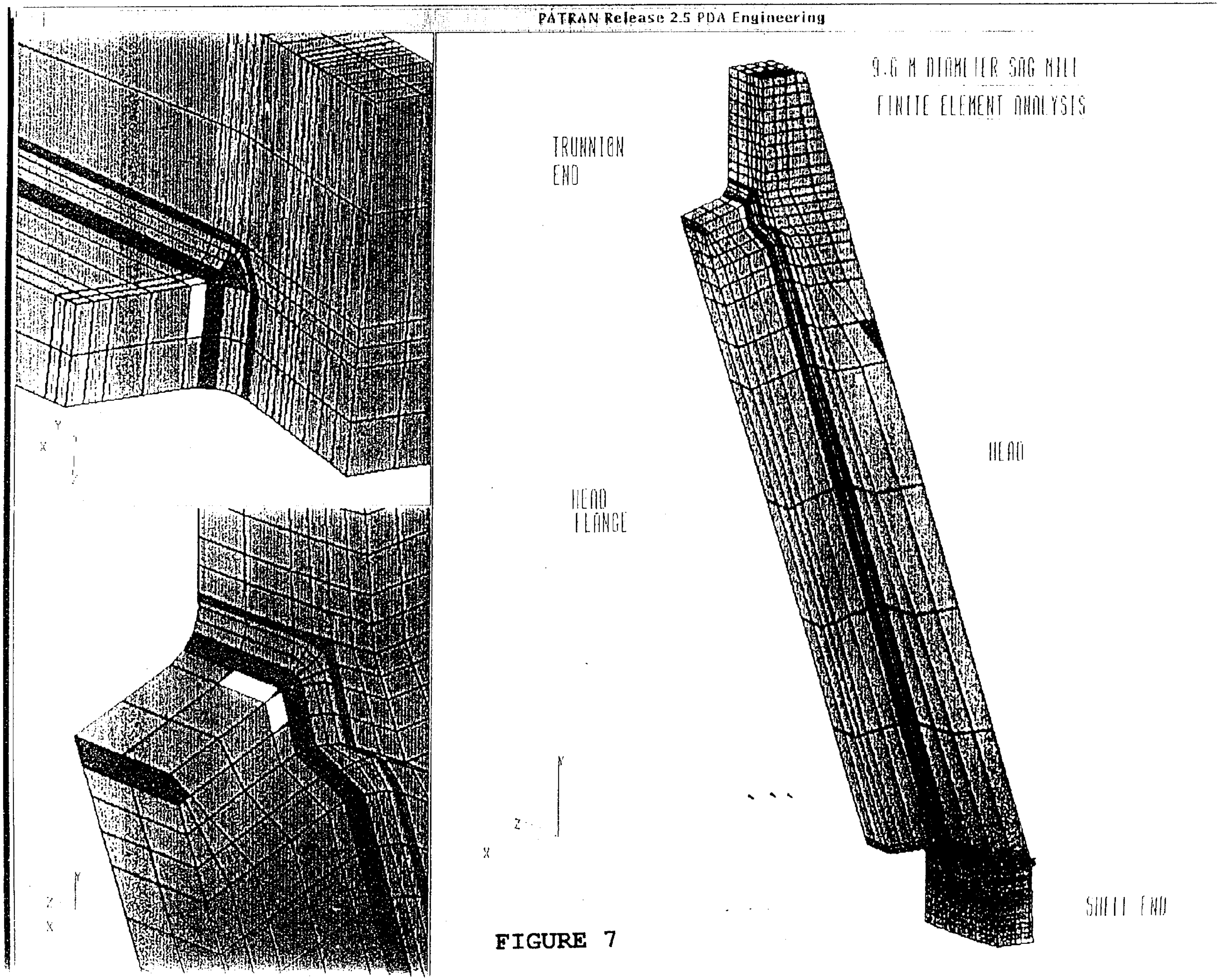

PATRAN Release 2.5 PDA Engineering
9.6 M DIAMETER SAG MILL
FINITE ELEMENT ANALYSIS
TRUNNION
END
HEAD
FLANGE
HEAD
SHELL END

FIGURE 7

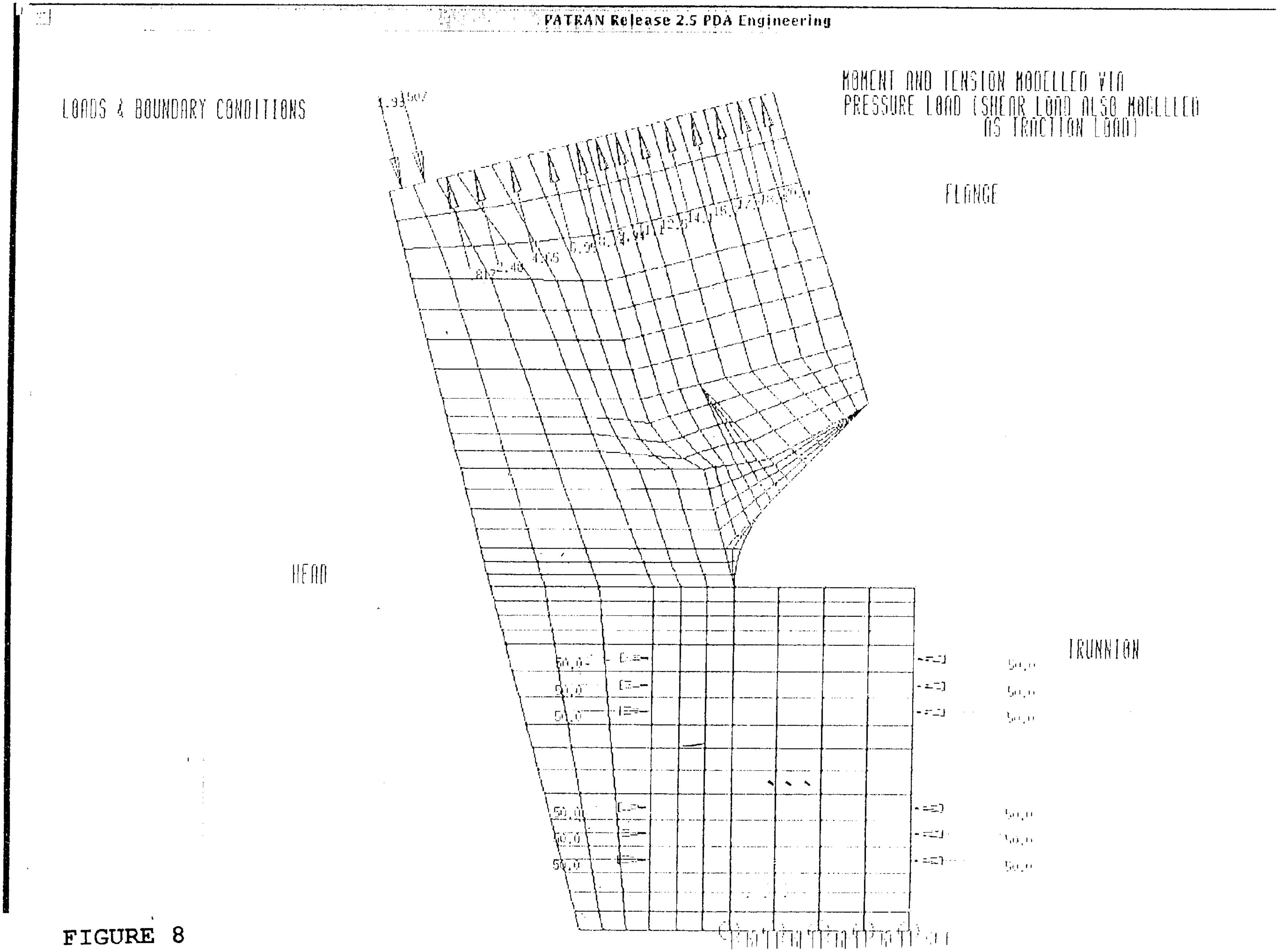
PATRAN Release 2.5 PDA Engineering
LOADS & BOUNDARY CONDITIONS
MOMENT AND TENSION MODELLED VIA
PRESSURE LOAD (SHEAR LOAD ALSO MODELLED
AS TRACTION LOAD)
FLANGE
HEAD
TRUNNION

FIGURE 8

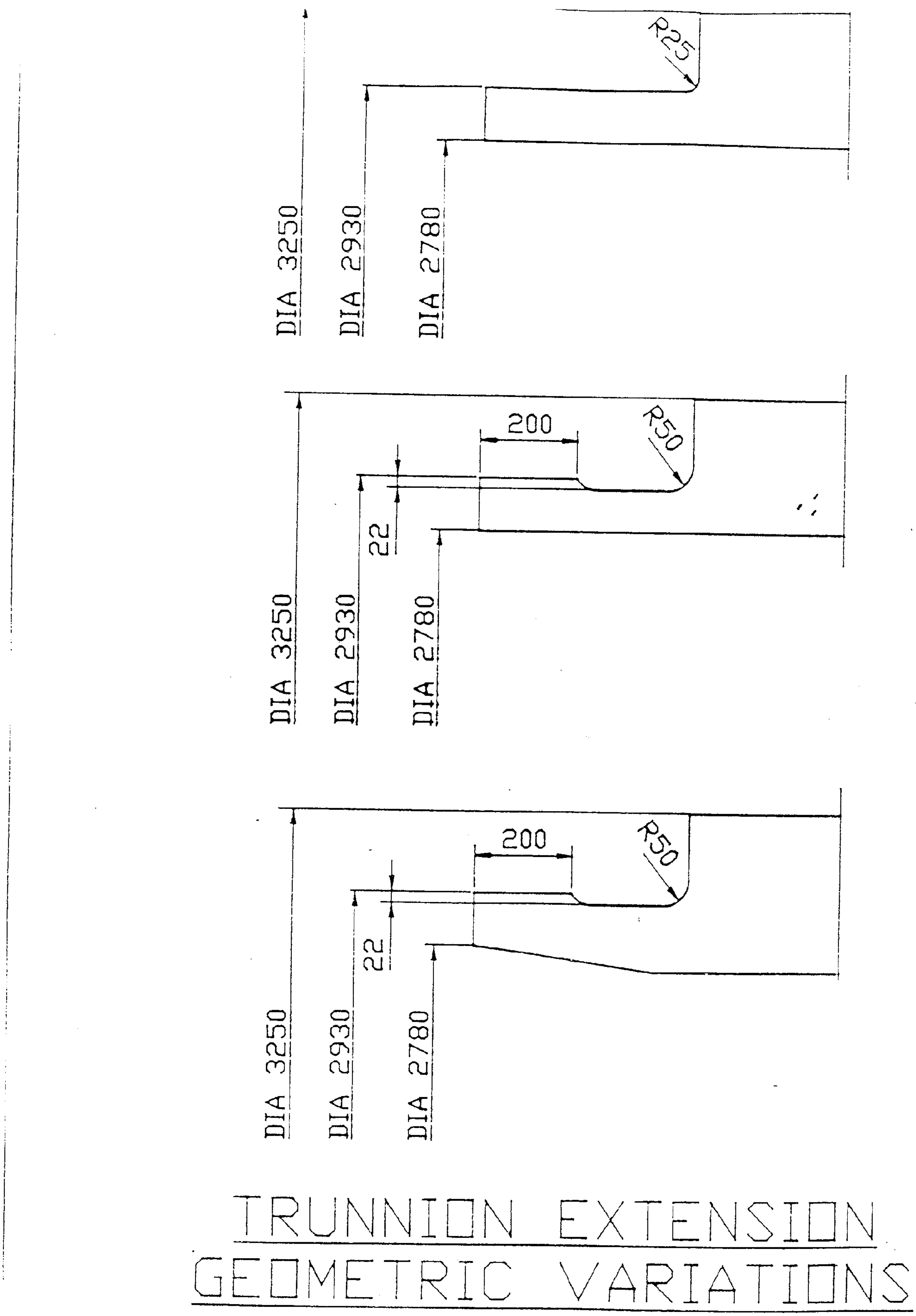
R25
DIA 3250
DIA 2930
DIA 2780
200
R50
22
DIA 3250
DIA 2930
DIA 2780
200
R50
22
DIA 3250
DIA 2930
DIA 2780
TRUNNION EXTENSION
GEOMETRIC VARIATIONS

FIGURE 9

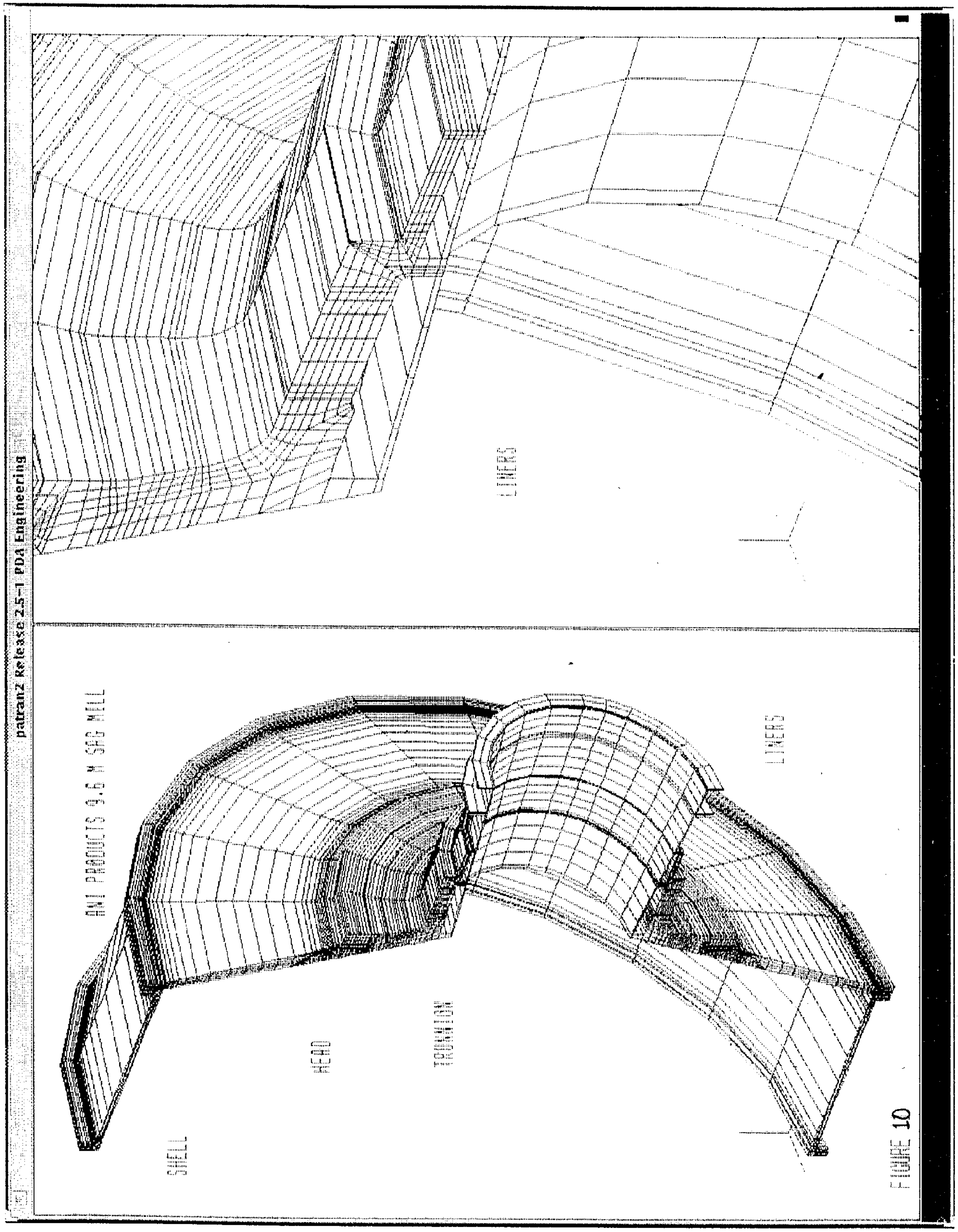
patran2 Release 2.5-1 PDA Engineering
ANI PRODUCTS 9.5 M SAG MILL
SHELL
HEAD
TRUNNION
LINERS
LINERS
FIGURE 10

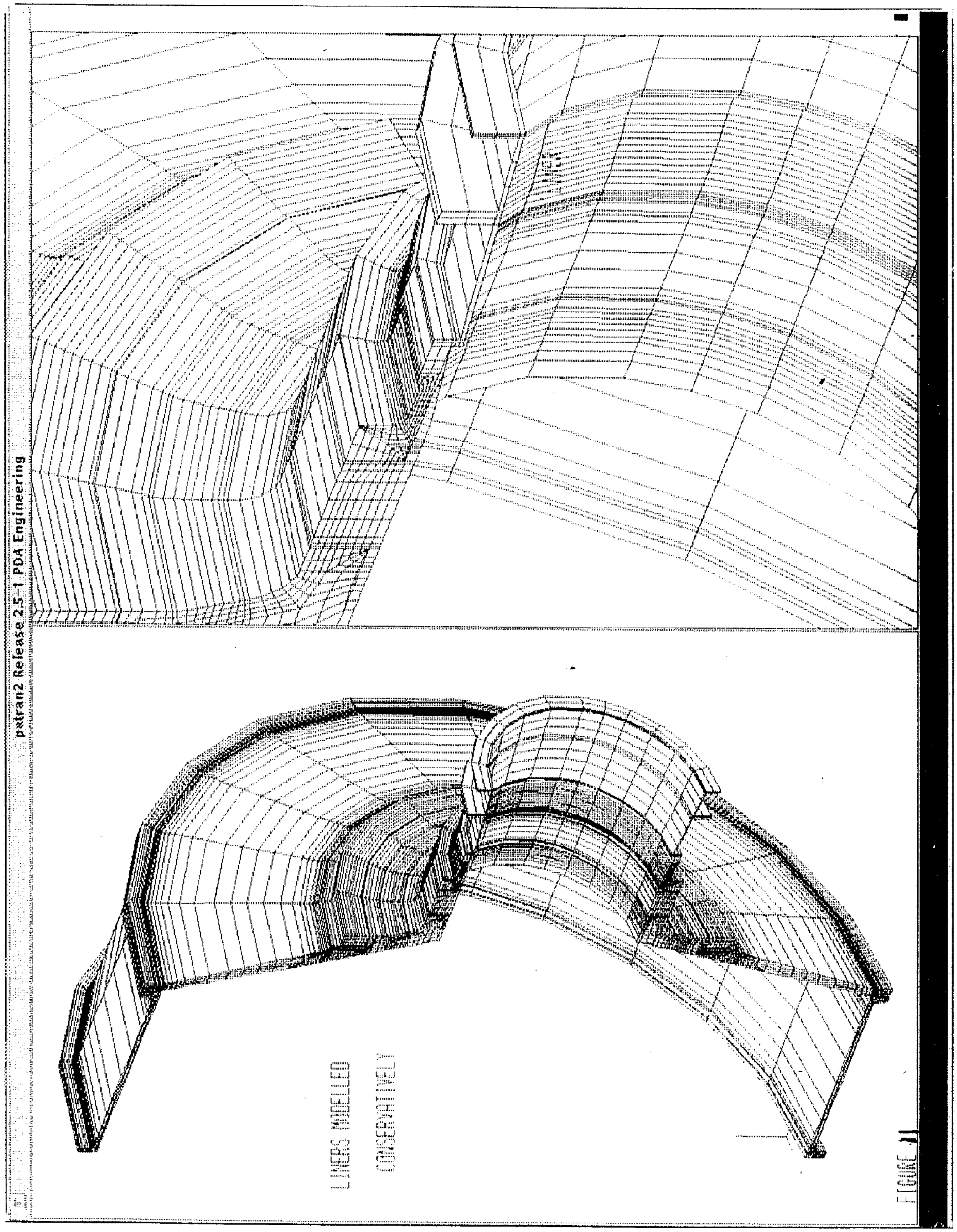
patran2 Release 2.5-1 PDA Engineering
LINERS MODELLED
CONSERVATIVELY
FIGURE 11

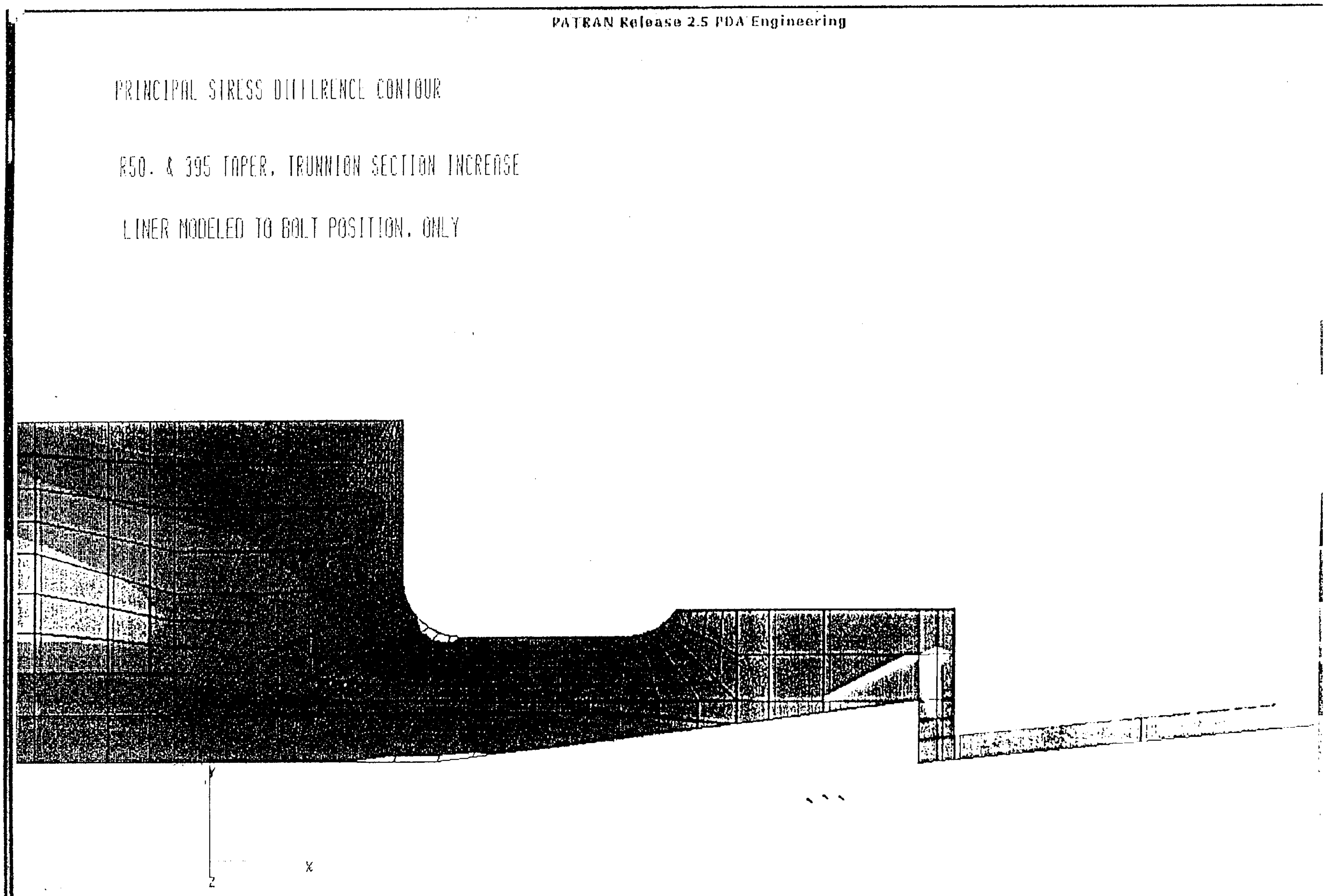
PATRAN Release 2.5 PDA Engineering
PRINCIPAL STRESS DIFFERENCE CONTOUR
R50. & 395 TAPER, TRUNNION SECTION INCREASE
LINER MODELED TO BOLT POSITION, ONLY
Y
X
Z

FIGURE 12

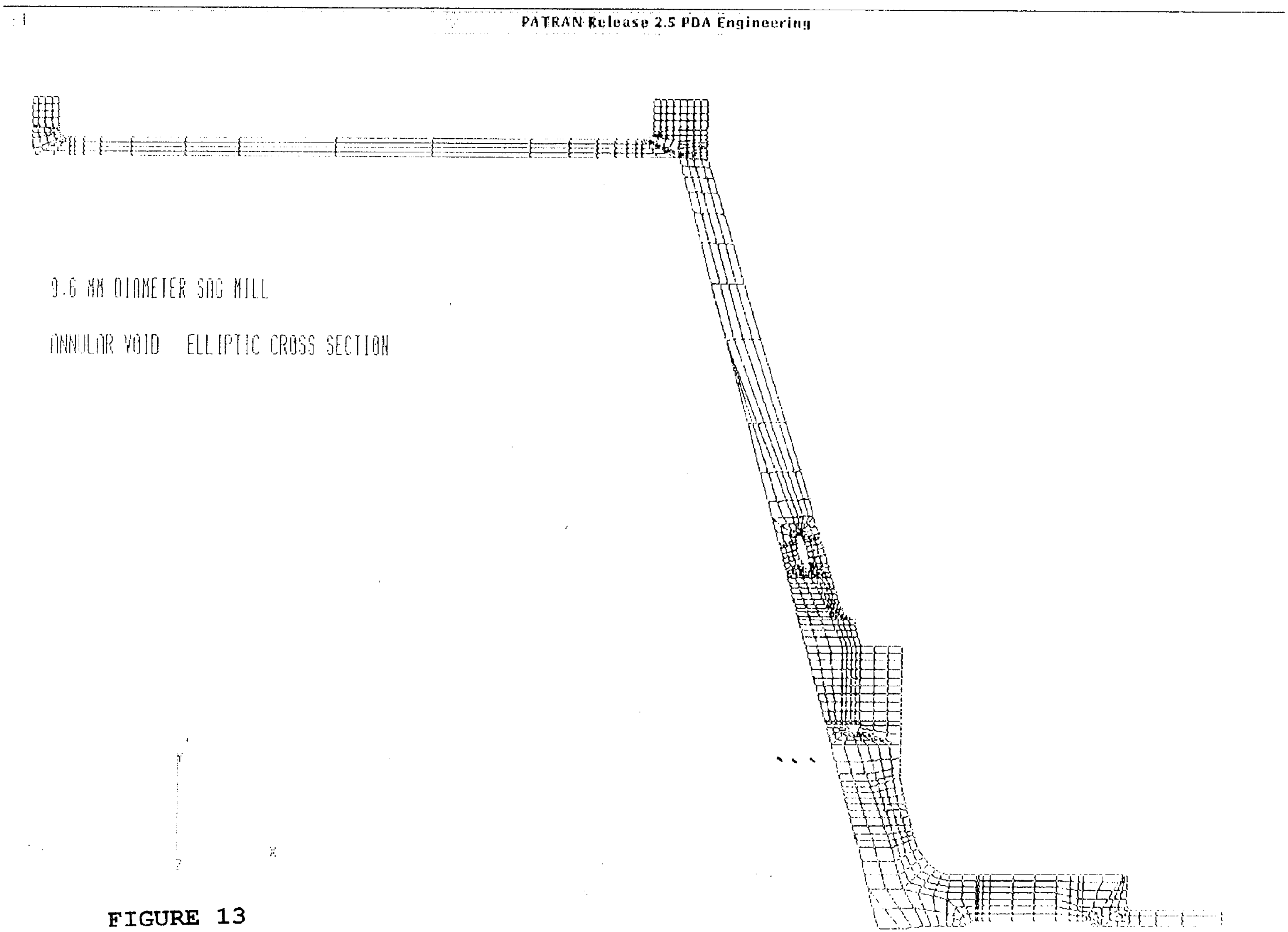
PATRAN Release 2.5 PDA Engineering
9.6 MM DIAMETER SAG MILL
ANNULAR VOID ELLIPTIC CROSS SECTION
Y
X

FIGURE 13

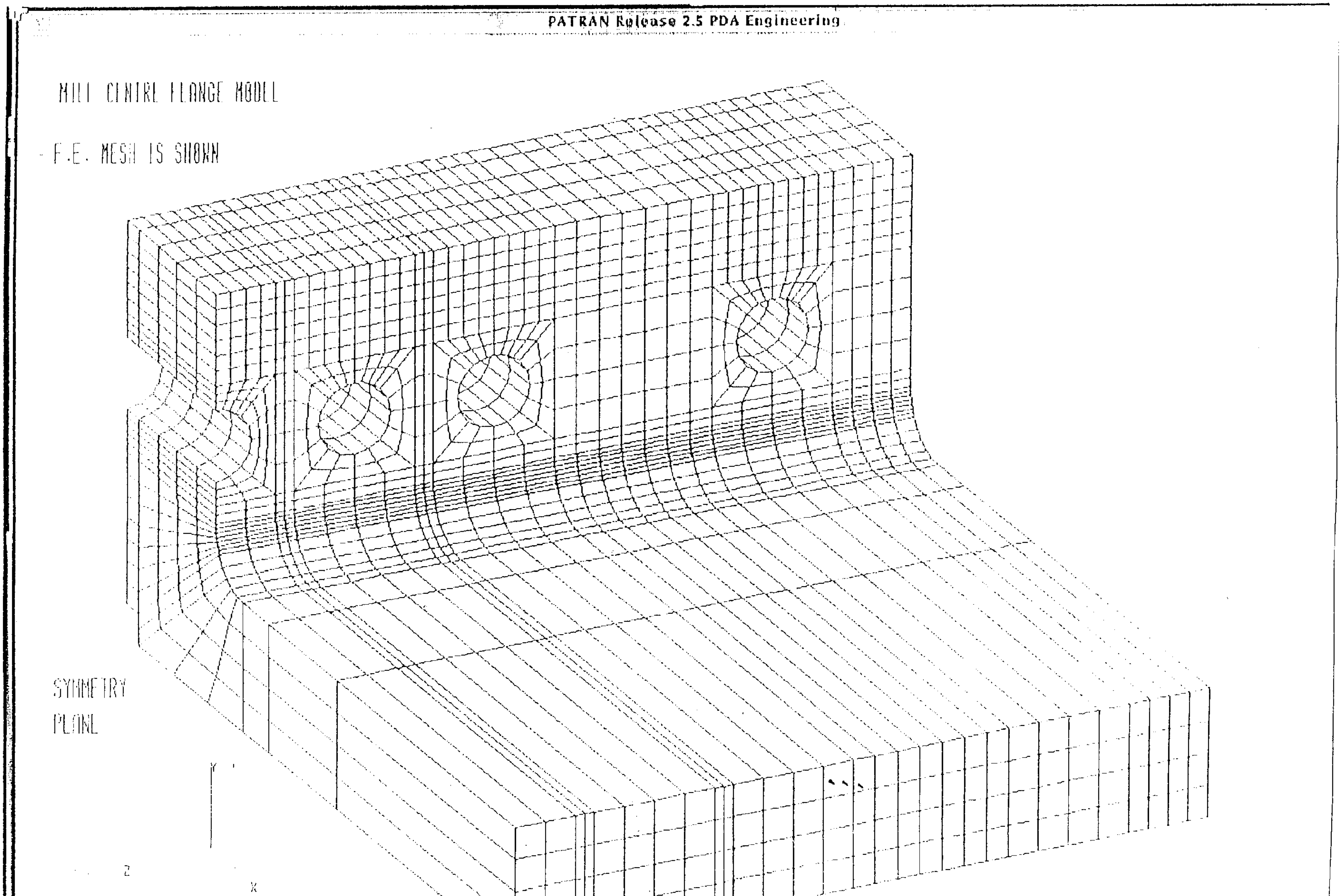
PATRAN Release 2.5 PDA Engineering
MILL CENTRE FLANGE MODEL
F.E. MESH IS SHOWN
SYMMETRY
PLANE
Y
Z
X

FIGURE 14